Acta Neuropathologica (2019) 138:827–835
https://doi.org/10.1007/s00401-019-02039-3

ORIGINAL PAPER

Routine RNA sequencing of formalin-fixed paraffin-embedded specimens in neuropathology diagnostics identifies diagnostically and therapeutically relevant gene fusions

Damian Stichel[1,2] · Daniel Schrimpf[1,2] · Belén Casalini[1,2] · Jochen Meyer[1,2] · Annika K. Wefers[1,2,3] · Philipp Sievers[1,2] · Andrey Korshunov[1,2,3] · Christian Koelsche[1,2,10] · David E. Reuss[1,2] · Annekathrin Reinhardt[1,2] · Azadeh Ebrahimi[1,2] · Francisco Fernández-Klett[1,2] · Tobias Kessler[4,5] · Dominik Sturm[3,6,7] · Jonas Ecker[3,7,9] · Till Milde[3,7,9] · Christel Herold-Mende[11] · Olaf Witt[3,7,9] · Stefan M. Pfister[3,6,7] · Wolfgang Wick[4,5] · David T. W. Jones[3,8] · Andreas von Deimling[1,2] · Felix Sahm[1,2,3]

Received: 8 May 2019 / Revised: 13 June 2019 / Accepted: 20 June 2019 / Published online: 5 July 2019

Abstract

Molecular markers have become pivotal in brain tumor diagnostics. Mutational analyses by targeted next-generation sequencing of DNA and array-based DNA methylation assessment with copy number analyses are increasingly being used in routine diagnostics. However, the broad variety of gene fusions occurring in brain tumors is marginally covered by these technologies and often only assessed by targeted assays. Here, we assessed the feasibility and clinical value of investigating gene fusions in formalin-fixed paraffin-embedded (FFPE) tumor tissues by next-generation mRNA sequencing in a routine diagnostic setting. After establishment and optimization of a workflow applicable in a routine setting, prospective diagnostic application in a neuropathology department for 26 months yielded relevant fusions in 66 out of 101 (65%) analyzed cases. In 43 (43%) cases, the fusions were of decisive diagnostic relevance and in 40 (40%) cases the fusion genes rendered a druggable target. A major strength of this approach was its ability to detect fusions beyond the canonical alterations for a given entity, and the unbiased search for any fusion event in cases with uncertain diagnosis and, thus, uncertain spectrum of expected fusions. This included both rare variants of established fusions which had evaded prior targeted analyses as well as the detection of previously unreported fusion events. While the impact of fusion detection on diagnostics is highly relevant, it is especially the detection of "druggable" fusions which will most likely provide direct benefit to the patients. The wider application of this approach for unbiased fusion identification therefore promises to be a major advance in identifying alterations with immediate impact on patient care.

Keywords RNA sequencing · Gene fusions · Molecular diagnostics · Molecular classification · Targeted treatment

Introduction

Molecular markers are of fundamental importance in neuropathology. The update of the WHO classification reflects this paradigmatic shift with the adoption of molecular parameters in the definition of entities [12]. Several of these markers are easily assessed, e.g., *IDH1*R132H, *BRAF*V600E, *H3F3A*K27M by immunohistochemistry, or other point mutations by Sanger sequencing. For a more comprehensive profiling, next-generation sequencing (NGS) panels have proven to be useful, e.g., for the range of mutations in medulloblastoma or diffuse glioma [9, 15]. Besides the analysis of the DNA sequence, the assessment of copy number variations, most prominently 1p/19q, but also *EGFR*,

Andreas von Deimling and Felix Sahm indicate shared senior authorship.

Electronic supplementary material The online version of this article (https://doi.org/10.1007/s00401-019-02039-3) contains supplementary material, which is available to authorized users.

✉ Andreas von Deimling
andreas.vondeimling@med.uni-heidelberg.de

✉ Felix Sahm
felix.sahm@med.uni-heidelberg.de

Extended author information available on the last page of the article

PTEN and others, is frequently needed and performed with a variety of methods. These include copy number information based on fluorescence in situ hybridization (FISH), multiplex ligation-dependent probe amplification (MLPA), or derived from array or NGS data. All of these analyses can be performed on formalin-fixed paraffin-embedded (FFPE) tissue or DNA extracted thereof.

Still, an emerging area of molecular alterations, particularly relevant for brain tumors, is so far underrepresented among the targets of established technologies: The wide variety of fusions that can drive brain tumor formation is only partially covered by these means. While the majority of *NAB2*:*STAT6* fusions can be detected by the nuclear reallocation of STAT6 protein in immunohistochemistry [20], *BRAF* fusion assessment depends on FISH or polymerase chain reaction (PCR) protocols in most laboratories. Particularly, the PCR approach is only directed against known, most common variants. Alternatively, structural variations can be inferred from array data. Our custom neurooncology NGS panel and some other diagnostically applied targeted DNA sequencing approaches are also capable of detecting a selection of the most common fusion events in a large percentage of cases [9, 19]. However, covering all possible variants with intronic DNA probes would require a design that overstretches a reasonable target size and would prevent efficient application in a routine setting.

Thus, rearrangements are not or only very selectively assessed in the routine molecular diagnostic work up. RNA sequencing covers all these structural aberrations. More recent approaches already employ targeted NGS panels for RNA sequencing. Sequencing for the entire mRNA, however, could detect even rare events without the limitations of a protocol limited to a pre-defined subset of fusions.

We here report on the application of full mRNA sequencing in FFPE-derived RNA for fusion detection in a diagnostic setting.

Methods

Tissue, DNA methylation analysis, DNA panel sequencing, and immunohistochemistry

The validation cohort was compiled from archival tissue for which ethical approval for research use was granted by local regulations. Selection criteria for samples that underwent diagnostic fusion detection by RNA sequencing are detailed below under "Prospective application in neuropathology diagnostics". DNA was extracted from tumors employing the Promega Maxwell 16 device. For DNA methylation analysis, genome-wide methylation patterns using the Illumina HumanMethylation 450 (450k) BeadChip (Illumina, San Diego, CA, USA) or the Infinium MethylationEPIC (850k) BeadChip (Illumina) array were analyzed. Processing of DNA methylation data was performed as previously described [6, 10]. For DNA panel sequencing, molecular barcode-indexed ligation-based sequencing libraries were constructed using 200 ng of sheared DNA. Libraries were enriched by hybrid capture with custom biotinylated RNA oligo pools covering exons of 130 cancer-associated genes [19]. Paired-end sequencing was performed using the NextSeq 500 (Illumina). Sequence data were mapped to the reference human genome using the Burrows–Wheeler Aligner and were processed using the publicly available SAM tools. Fusion calling was performed using deFuse, Arriba and TopHat (as for RNA sequencing data, see below for details). Immunohistochemistry for STAT6 was performed according to the published protocol [20].

RNA sequencing protocol

The protocol for RNA sequencing comprises the following steps: from samples with sufficient tumor cell content (> 60% based on H&E inspection), RNA was extracted using the Maxwell 16 LEV RNA FFPE Kit (catalogue # AS1260, Promega) on a Maxwell 16 Instrument (AS2000, Promega) following the manufacturer's instructions. The RNA concentrations were measured on a Fluorometer "FLUOStar Omega" (BMG Labtech) with the Invitrogen Qubit RNA BR Assay Kit (Q10210, Thermo Fisher Scientific). The DV_{200} value (the percentage of fragments > 200 nucleotides) of each sample was calculated with the Agilent RNA 6000 Nano Kit (catalogue # 5067-1511, Agilent Technologies) on an Agilent 2100 Bioanalyzer (catalogue # G2939A, Agilent Technologies), since it determines the input amount for the following steps according to the protocol. Next, libraries were prepared using the TruSeq RNA Library Prep for Enrichment kit (catalogue # 20020189, Illumina) and enriched with the TruSeq RNA Enrichment kit (catalogue # 20020490, Illumina). The 45 Mb spanning Exome Panel (catalogue # 20020183) was applied. For demultiplexing index, adapters were added [TruSeq RNA Single Indexes Set A/Set B (12 Indexes each, catalogue # A: 20020492, B: 20020493)]. Subsequently, the quality of a library was controlled on a Agilent 2100 Bioanalyzer (G2939A, Agilent Technologies) using the Agilent DNA 1000 Kit (5067-1504, Agilent Technologies) and the Agilent High Sensitivity DNA Kit (catalogue #5067-4626, Agilent Technologies). Sequencing was performed on a NextSeq 500 instrument (Illumina) with 75 bp 'paired-end' sequencing technology employing high-output flow cells. The mean number of reads per sample and lane in two representative libraries was 6,189,514 (range: 1,911,295–13,212,770). The sequencing procedure for one library took roughly 18 h and generated raw data files in binary base call (bcl) format. The pipeline is schematically depicted in Fig. 1.

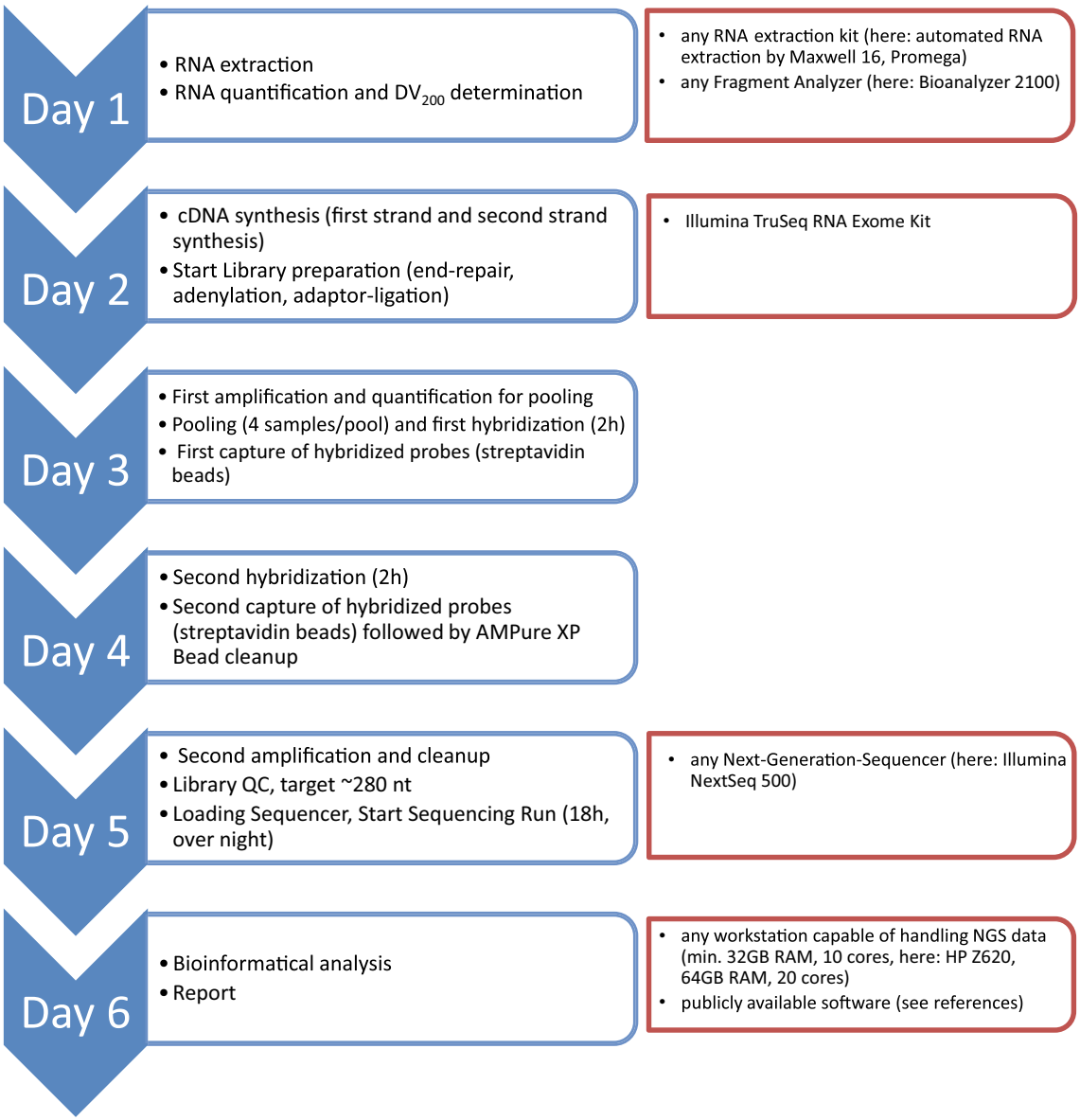

Fig. 1 Workflow for RNA sequencing in neuropathology diagnostics: flow chart of the protocol steps and involved equipment

Bioinformatics specific for RNA sequencing data

After sequencing, the raw data were stored on a "network attached storage" (NAS) server and for analysis copied locally to a workstation. First, the bcl files were converted into fastq format using the tool "bcl2fastq" by Illumina, demultiplexed and trimmed to remove index adapter sequences. To check the quality of the sequencing results, the fastq files were further processed using the tool fastqc. The independent tools deFuse [13], TopHat [8] and Arriba (https://github.com/suhrig/arriba) were applied to the fastq files to detect fusions in the data. Standard settings were applied for all three tools and reads were aligned to the Genome Reference Consortium Human Build 37 (GRCh37).

Results

Diagnostically relevant gene fusions can be detected from FFPE RNA sequencing data

First, we wanted to test if diagnostically relevant fusions in FFPE samples can be detected from RNA sequencing data. We thus first compiled a validation set of 15 cases with known fusions as detected by other methods before (Table 1). To develop widely applicable pipelines for fusion calling, we used the publicly available tools deFuse [13], TopHat [8] and Arriba (https://github.com/suhrig/arriba) and compared their performance. The workflow is depicted in Fig. 1. Among the three tested algorithms, Arriba

Table 1 Fusion calling of index fusions in validation set

ID	Diagnosis	Corresponding method	Fusion partners	Number of reads	Arriba	deFuse	TopHat
1	Pilocytic astrocytoma WHO grade I	850 k CNP	KIAA1549:BRAF	25,922,949	No	No	No
2	Pilocytic astrocytoma WHO grade I	850 k CNP	KIAA1549:BRAF	15,459,469	No	No	No
3	Pilocytic astrocytoma WHO grade I	850 k CNP	KIAA1549:BRAF	23,120,410	No	No	No
4	Pilocytic astrocytoma WHO grade I	850 k CNP	KIAA1549:BRAF	31,181,465	Yes (3)	No	No
5	Pilocytic astrocytoma WHO grade I	850 k CNP	KIAA1549:BRAF	29,541,677	Yes (5)	No	No
6	HGNET MN1	850 k CNP	MEN1:BEND2	9,641,586	Yes (3)	No	Yes (8)
7	HGNET MN1	850 k CNP	MEN1:BEND2	18,678,877	Yes (6)	Yes (44)	Yes (35)
8	Solitary fibrous tumor/hemangiopericytoma	STAT6 staining	NAB2:STAT6	22,036,275	Yes (28)	No	Yes (59)
9	Solitary fibrous tumor/hemangiopericytoma	STAT6 staining	NAB2:STAT6	2,501,812	Yes (8)	Yes (114)	Yes (35)
10	Solitary fibrous tumor/hemangiopericytoma	STAT6 staining	NAB2:STAT6	22,363,680	Yes (13)	No	Yes (27)
11	Ependymoma RELA positive	850 k CNP	c11orf95:RELA	47,266,331	Yes (13)	Yes (34)	Yes (10)
12	Ependymoma RELA positive	850 k CNP	c11orf95:RELA	55,572,246	Yes (5)	No	No
13	Ependymoma RELA positive	850 k CNP	c11orf95:RELA	40,035,859	Yes (2)	No	No
14	Ependymoma RELA positive	850 k CNP	c11orf95:RELA	38,874,441	Yes (2)	No	No
15	Ependymoma RELA positive	850 k CNP	c11orf95:MAML2	20,440,278	Yes (3)	No	No

Cases in the validation set of samples with established fusion events based on another method as indicated. Three fusion detection algorithms were used: Arriba, deFuse, and TopHat. The columns "Arriba", "deFuse", and "TopHat" indicate whether the fusion event was detected with the respective tool. CNP: copy number plot, HGNET: high-grade neuroepithelial tumor with MN1 alteration. Total number of reads for the case and number of supporting reads per tool (in parentheses) are given

Table 2 Sensitivity and computation time

Tool	No of called fusions per sample in filtered output				Average computing time per sample (h)
	Min	Max	Average	SD	
Arriba	2	90	25.08	24.38	0:12
deFuse	1	215	39.16	53.96	7:58
TopHat	0	8	1.62	2.39	6:40

Specifications on average number of proposed fusion calls in a representative library and the computation time for the three assessed tools

SD standard deviation, *min* minimum, *max* maximum

emerged as the most reliable and efficient tool (Tables 1, 2) and reached a sensitivity of 80% in the validation set. Intriguingly, the only missed fusion event with Arriba was *KIAA1549:BRAF*. However, the algorithms also proposed numerous additional fusion calls of unknown significance (Table 2, Fig. 2).

Prospective application in neuropathology diagnostics

Based on the findings that RNA sequencing from FFPE can detect a considerable fraction of relevant fusions in brain tumors, we prospectively applied this method in diagnostics for selected cases. Between June 2016 and October 2018, 101 diagnostic samples were assessed (Fig. 3, Online Resource 1: Supplementary Table 1). No strict inclusion criteria were applied. Typically, RNA sequencing was triggered in two scenarios: first, in cases with an unclear diagnosis, if a fusion was suspected due to one of the histologically considered differential diagnoses and/or brain tumor classifier result [3], and if detection of a fusion was regarded as potentially useful in finalizing the diagnosis. This pattern to include particularly challenging cases enriched the cohort for samples without a clear-cut WHO diagnosis. Second, RNA sequencing was initiated if the diagnosis was already rendered but definite detection of a certain associated fusion had further clinical implications.

Relevant fusions were detected in $n = 66/101$ cases (65.3%, Fig. 3). Relevance of fusions among the proposed calls was determined by taking into account (a) the confidence prediction of the Arriba algorithm, (b) whether the proposed fusion call results in a functional protein based on the included protein domains and sequence, (c) affected pathways and biological relevance in the considered differential diagnoses. Among the cases with identified relevant fusion, the largest group with 32 samples consisted of cases that histologically were compatible with the spectrum of low-grade glial/glioneuronal tumors. In these, however, no indications for the most prevalent alterations (including *BRAF* mutations or fusions and *FGFR1* mutations) had been detected before with panel sequencing and 850 k array. Additionally, fusions were identified in 18 sarcomas, 11 diffuse high-grade diffuse gliomas, and 5 cases of mixed other entities. The detected fusions were integrated with the histology and other available molecular data (e.g., indications of breakpoints from 850 k and DNA sequencing data, Online Resource 1: Supplementary Fig. 1) and yielded diagnostic

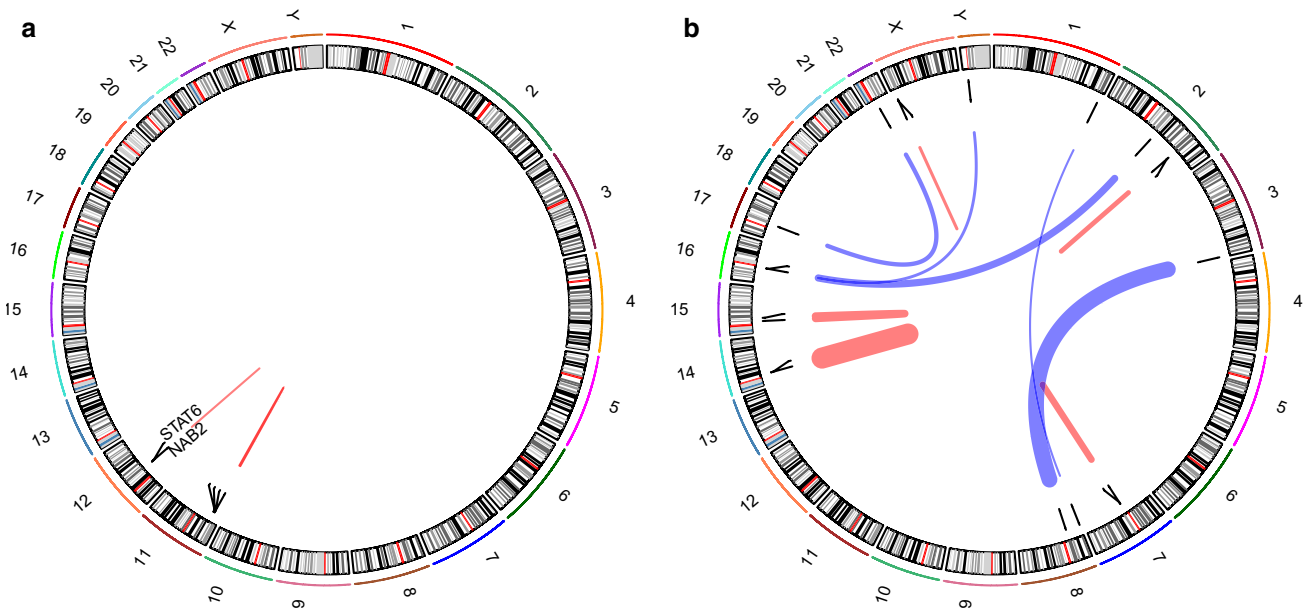

Fig. 2 Illustration of differing results of fusion calling tools: fusion calls proposed by Arriba (left) and deFuse (right) in a case with proven NAB2:STAT6 fusion. Red lines refer to intrachromosomal fusions and blue lines refer to interchromosomal fusions. The width of the lines refers to the number of supporting reads

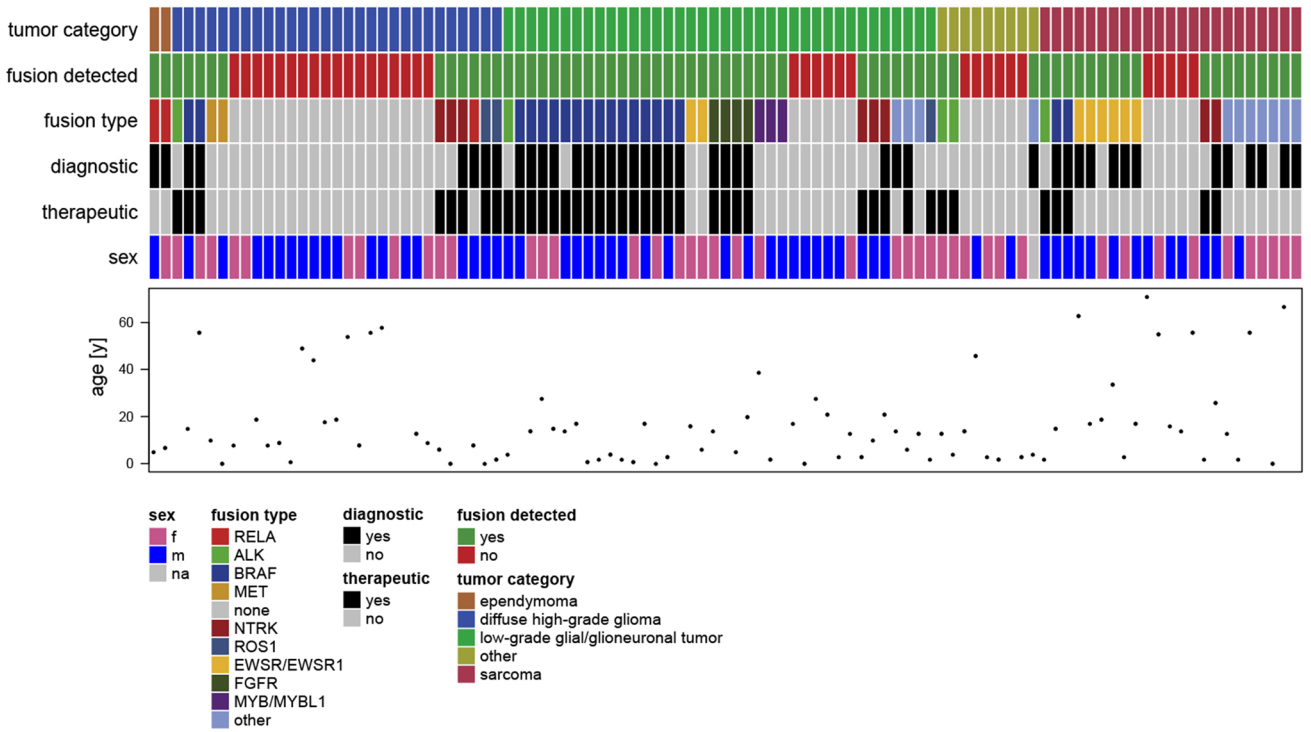

Fig. 3 Prospective cohort: characteristics of the 101 included diagnostic cases and identified fusions. f: female, m: male, na: information not available, diagnostic—detected fusion was of relevance for tumor classification, therapeutic—detected fusion represents a clinically relevant target

insight in 43/101 cases (42.6%). This mostly applied to fusions in the MAPK pathway for identification or confirmation of suspected pilocytic astrocytoma or pleomorphic xanthoastrocytoma, or pathognomonic fusions in sarcoma, e.g., EWSR fusion variants. In 40/101 cases (39.6%), the detected fusions even provided a target for treatment: MAPK pathway targets, amenable by MEK inhibitors were most frequent (19 of 40 therapeutically relevant fusions involving *BRAF*, 47.5%, and one involving *RAF1*), followed by equal numbers of targets for TRK inhibitors with involvement of *NTRK1/2/3* or *ROS1*/*ALK* pathway inhibitors, respectively (each 8/40, 20%), and *FGFR* alterations in 4/40 cases (10%).

Three examples are given in Fig. 4: first, a 5-year-old girl in whom initially a pilomyxoid astrocytoma WHO grade II (based on the 2007 classification) was diagnosed. Additional analyses were requested as the tumor progressed despite radiation. 850 k analysis revealed the methylation class pilocytic astrocytoma of the midline, but both 850 k and panel sequencing did not identify the driving alteration. RNA sequencing detected a *QKI*:*RAF1* fusion (Fig. 2a).

The second case was a 32-year-old man with a pilocytic astrocytoma WHO grade I diagnosed at the age of 29. The tumor progressed despite radiation and a second resection was performed. Since no driver alteration was identified with 850 k and panel sequencing, a RNA sequencing was performed and revealed a *DMD*:*NTRK2* fusion (Fig. 2b).

Third, a 2-year-old boy was histologically diagnosed with a glioblastoma IDH wildtype WHO grade IV. DNA methylation analysis revealed the methylation class infantile hemispheric glioma, an entity included in the Heidelberg brain tumor classifier but so far not in the WHO classification. Histologically, these tumors are typically compatible with glioblastoma. The copy number profile (CNP) derived from the 850 k analysis suggested several focal deletions. *ALK* and *ROS1* fusions, both potentially therapeutically relevant, are frequent in this entity, and the ROS1 locus was among the altered regions in the CNP. RNA sequencing was performed and revealed an *ARCN1*:*ROS1* fusion (Fig. 2c).

All three examples show that the fusion event is within the spectrum of pathway activations known for the respective entity, further substantiating the diagnosis, and provide actionable targets, in these cases for MEK, NTRK, or ROS inhibitors, respectively.

Discussion

We here demonstrated the feasibility of RNA sequencing from FFPE-derived RNA in a diagnostic routine setting. Collectively, our data show that RNA sequencing has great potential to inform about diagnostically and therapeutically relevant alterations in brain tumors. The ability to reliably perform the analysis on RNA derived from FFPE greatly increases the amount of cases which can undergo this testing.

While the current WHO classification has introduced many molecular markers, most of them are point mutations or copy number changes. With the emerging use of RNA and whole genome sequencing, novel fusions that are pathognomonic for previously only histologically defined, or even not yet recognized entities have been reported. This includes fusion events or tandem duplications, respectively, involving *FOXR2*, *MN1*, *BCOR*, or *CIC* in novel entities previously subsumed under the term "primitive neuroectodermal tumor" [21], *MYB* fusions in angiocentric glioma [1, 4], or *FGFR* and *NTRK* fusions in other low-grade glial/glioneuronal tumor [7, 18]. For papillary glioneuronal tumors, a novel potentially entity-defining recurrent fusion involving *PRKCA* has been reported [2, 5, 14, 16]. This technology now allows the routine assessment of this increasing amount of diagnostically relevant parameters in a standardized, comprehensive manner.

Since this study included diagnostic cases that already underwent several other analyses before (e.g., reference histology, DNA methylation array, DNA panel sequencing) and these were inconclusive or even encouraged the search for a gene fusion in absence of other driving alterations, the rate of fusion-positive cases is certainly increased compared to an average cohort of surgical neuropathology specimen.

In our experience, enriching the cases tested for fusions particularly with those that are diagnostically challenging may also result in the situation that a clinically relevant alteration is found, but a clear-cut diagnosis can still not be rendered since the case may—despite fusion detection—not be compatible with the diagnostic criteria of any established entity. Regularly applying this method in otherwise unresolvable cases thus holds potential to reveal not only novel, as of yet unknown, fusion events, but also contribute to the delineation of further novel tumor classes and subgroups.

However, the approach has also technical limitations. The detection rate in the validation set was only 80%.

Of note, the *KIAA1549:BRAF* fusion transcript, which was the only validation target that accounted for the suboptimal detection rate, seems to be generally expressed at low levels (authors' unpublished data). This was also reported in a study by Tomic et al. [22], and another study had previously shown that the fusion transcript itself is expressed at lower levels than *BRAF* [11]. In our data, the cases in which no *KIAA1549:BRAF* was found had no significantly inferior read count than the other samples with detected *BRAF* fusion or other fusions (Table 1). Of note, in two of the three cases in which the *KIAA1549:BRAF* fusion was not detected, a *KIAA1549:BRAF* fusion could be inferred using the 'grep' command to search the fastq files for known breakpoint sequences (as proposed in [17]). In fact, in these two cases, the fusion was originally detected by Arriba, however, with

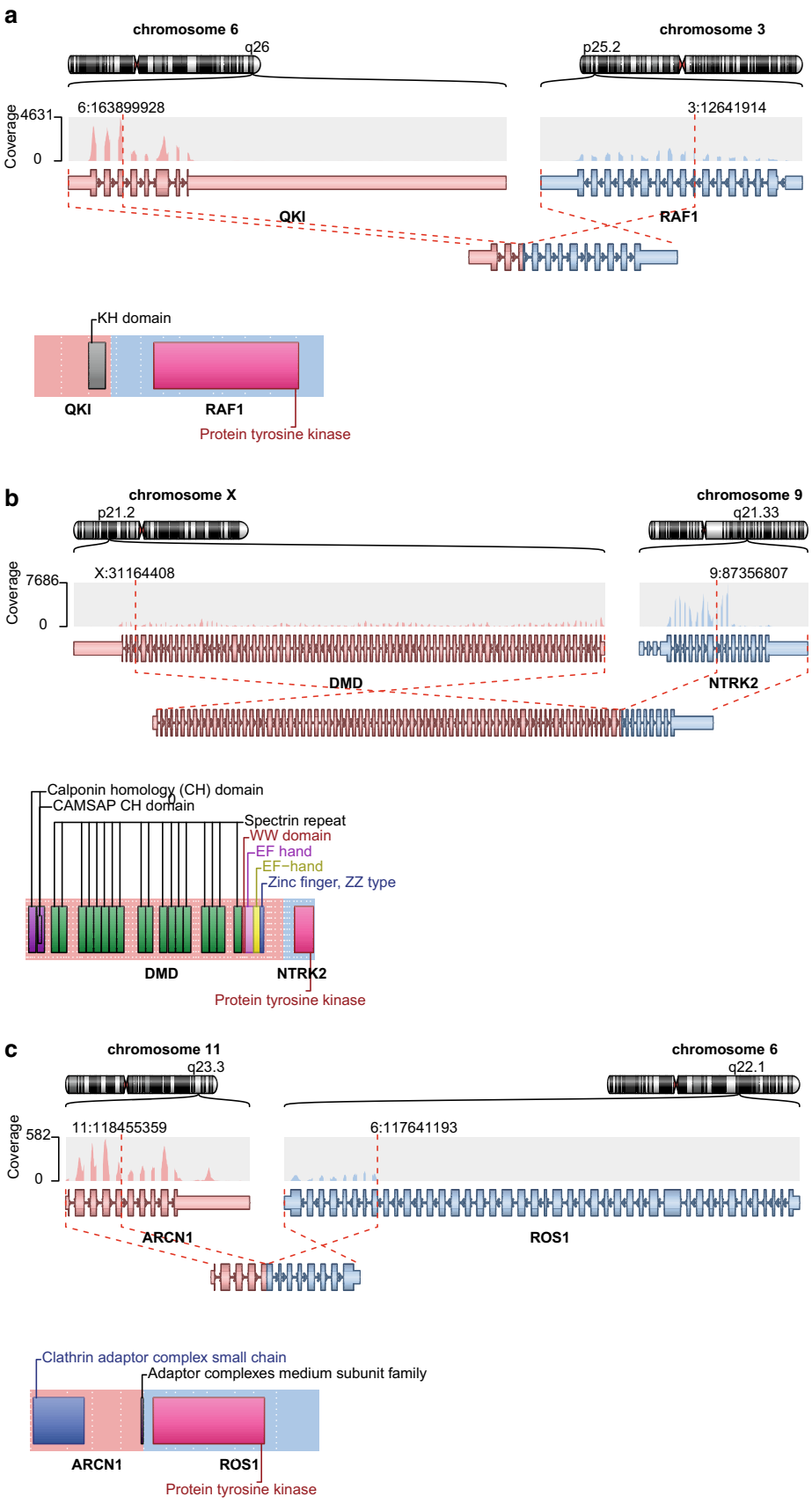

Fig. 4 Representative cases: illustration of exact fusion configuration of three representative diagnostic samples. The chromosomal position is depicted and annotated and the resulting fusion gene illustrated. Demonstration of the involved protein domains, also included in the diagnostic reports, supports interpretation of the relevance

only one supporting read and thus was discarded from the results by the algorithm.

The algorithms propose many fusions that have to be manually inspected for relevance and that due to their number cannot feasibly be verified or falsified via PCR. However, cases in which full mRNA fusion assessment is performed had typically undergone a series of molecular analyses before allowing integrating the RNA sequencing data into already available information about possible breakpoints from copy number plots (Online Resource 1: Supplementary Fig. 1), or differential sequence coverage of exons involved in the fusion event vs those not affected, and soft-clipped reads supporting the rearrangement. Thus, we did not apply additional FISH or PCR verification of the fusions presented here, but integrated the RNA sequencing data with other already available molecular information, and validated the findings in context of histology and clinical data. If no supporting information, e.g., about possible breakpoints, is available, or a particular fusion may even be detected in an entity for which it is uncommon or even unprecedented, additional verification is certainly recommendable. With the emergence of NGS approaches to molecular diagnostics, the application of "directed" methods as FISH or PCR will, however, probably further decrease. For now, these still provide a cost-effective alternative if the suspected alteration is clearly rendered.

In contrast to these technologies, our approach is unbiased in that regard that it does not target a pre-defined set of genes, thereby also differing from currently emerging RNA sequencing panels, but is still restricted to those mRNA fragments captured by the included probes.

In summary, we have shown that this comprehensive mRNA sequencing approach can be routinely applied to diagnostic FFPE samples. We demonstrated that this analysis can provide substantial insight into the biology of otherwise diagnostically unresolvable cases and identify immediately "druggable" treatment targets.

Acknowledgements We thank Hai Yen Nguyen, Laura Dörner, and Lisa Kreinbihl for skillful technical assistance. This study was supported by the Else Kröner-Fresenius Stiftung (EKFS, 2017_EKES.24) and the Pediatric Low Grade Astrocytoma Fund (PLGA Fund) at the Pediatric Brain Tumor Foundation (PBTF).

References

1. Bandopadhayay P, Ramkissoon LA, Jain P, Bergthold G, Wala J, Zeid R et al (2016) MYB-QKI rearrangements in angiocentric glioma drive tumorigenicity through a tripartite mechanism. Nat Genet 48:273–282. https://doi.org/10.1038/ng.3500
2. Bridge JA, Liu XQ, Sumegi J, Nelson M, Reyes C, Bruch LA et al (2013) Identification of a novel, recurrent SLC44A1-PRKCA fusion in papillary glioneuronal tumor. Brain Pathol 23:121–128. https://doi.org/10.1111/j.1750-3639.2012.00612.x
3. Capper D, Jones DTW, Sill M, Hovestadt V, Schrimpf D, Sturm D et al (2018) DNA methylation-based classification of central nervous system tumours. Nature 555:469–474. https://doi.org/10.1038/nature26000
4. Chan E, Bollen AW, Sirohi D, Van Ziffle J, Grenert JP, Kline CN et al (2017) Angiocentric glioma with MYB-QKI fusion located in the brainstem, rather than cerebral cortex. Acta Neuropathol 134:671–673. https://doi.org/10.1007/s00401-017-1759-x
5. Hou Y, Pinheiro J, Sahm F, Reuss DE, Schrimpf D, Stichel D et al (2019) Papillary glioneuronal tumor (PGNT) exhibits a characteristic methylation profile and fusions involving PRKCA. Acta Neuropathol. https://doi.org/10.1007/s00401-019-01969-2
6. Hovestadt V, Remke M, Kool M, Pietsch T, Northcott PA, Fischer R et al (2013) Robust molecular subgrouping and copy-number profiling of medulloblastoma from small amounts of archival tumour material using high-density DNA methylation arrays. Acta Neuropathol 125:913–916. https://doi.org/10.1007/s00401-013-1126-5
7. Jones DT, Hutter B, Jager N, Korshunov A, Kool M, Warnatz HJ et al (2013) Recurrent somatic alterations of FGFR1 and NTRK2 in pilocytic astrocytoma. Nat Genet 45:927–932. https://doi.org/10.1038/ng.2682
8. Kim D, Pertea G, Trapnell C, Pimentel H, Kelley R, Salzberg SL (2013) TopHat2: accurate alignment of transcriptomes in the presence of insertions, deletions and gene fusions. Genome Biol 14:R36. https://doi.org/10.1186/gb-2013-14-4-r36
9. Kline CN, Joseph NM, Grenert JP, van Ziffle J, Talevich E, Onodera C et al (2017) Targeted next-generation sequencing of pediatric neuro-oncology patients improves diagnosis, identifies pathogenic germline mutations, and directs targeted therapy. Neuro Oncol 19:699–709. https://doi.org/10.1093/neuonc/now254
10. Korshunov A, Ryzhova M, Hovestadt V, Bender S, Sturm D, Capper D et al (2015) Integrated analysis of pediatric glioblastoma reveals a subset of biologically favorable tumors with associated molecular prognostic markers. Acta Neuropathol 129:669–678. https://doi.org/10.1007/s00401-015-1405-4
11. Lin A, Rodriguez FJ, Karajannis MA, Williams SC, Legault G, Zagzag D et al (2012) BRAF alterations in primary glial and glioneuronal neoplasms of the central nervous system with identification of 2 novel KIAA1549:BRAF fusion variants. J Neuropathol Exp Neurol 71:66–72. https://doi.org/10.1097/NEN.0b013e31823f2cb0
12. Louis DN, Perry A, Reifenberger G, von Deimling A, Figarella-Branger D, Cavenee WK et al (2016) The 2016 world health organization classification of tumors of the central nervous system: a summary. Acta Neuropathol 131:803–820. https://doi.org/10.1007/s00401-016-1545-1
13. McPherson A, Hormozdiari F, Zayed A, Giuliany R, Ha G, Sun MG et al (2011) deFuse: an algorithm for gene fusion discovery in tumor RNA-Seq data. PLoS Comput Biol 7:e1001138. https://doi.org/10.1371/journal.pcbi.1001138
14. Nagaishi M, Nobusawa S, Matsumura N, Kono F, Ishiuchi S, Abe T et al (2016) SLC44A1-PRKCA fusion in papillary and rosette-forming glioneuronal tumors. J Clin Neurosci 23:73–75. https://doi.org/10.1016/j.jocn.2015.04.021
15. Nikiforova MN, Wald AI, Melan MA, Roy S, Zhong S, Hamilton RL et al (2016) Targeted next-generation sequencing panel (GlioSeq) provides comprehensive genetic profiling of central nervous system tumors. Neuro Oncol 18:379–387. https://doi.org/10.1093/neuonc/nov289
16. Pages M, Lacroix L, Tauziede-Espariat A, Castel D, Daudigeos-Dubus E, Ridola V et al (2015) Papillary glioneuronal tumors: histological and molecular characteristics and diagnostic value of SLC44A1-PRKCA fusion. Acta Neuropathol Commun 3:85. https://doi.org/10.1186/s40478-015-0264-5

17. Panagopoulos I, Gorunova L, Bjerkehagen B, Heim S (2014) The "grep" command but not FusionMap, FusionFinder or ChimeraScan captures the CIC-DUX4 fusion gene from whole transcriptome sequencing data on a small round cell tumor with t(4;19)(q35;q13). PLoS One 9:e99439. https://doi.org/10.1371/journal.pone.0099439
18. Qaddoumi I, Orisme W, Wen J, Santiago T, Gupta K, Dalton JD et al (2016) Genetic alterations in uncommon low-grade neuroepithelial tumors: BRAF, FGFR1, and MYB mutations occur at high frequency and align with morphology. Acta Neuropathol 131:833–845. https://doi.org/10.1007/s00401-016-1539-z
19. Sahm F, Schrimpf D, Jones DT, Meyer J, Kratz A, Reuss D et al (2016) Next-generation sequencing in routine brain tumor diagnostics enables an integrated diagnosis and identifies actionable targets. Acta Neuropathol 131:903–910. https://doi.org/10.1007/s00401-015-1519-8
20. Schweizer L, Koelsche C, Sahm F, Piro RM, Capper D, Reuss DE et al (2013) Meningeal hemangiopericytoma and solitary fibrous tumors carry the NAB2-STAT6 fusion and can be diagnosed by nuclear expression of STAT6 protein. Acta Neuropathol 125:651–658. https://doi.org/10.1007/s00401-013-1117-6
21. Sturm D, Orr BA, Toprak UH, Hovestadt V, Jones DT, Capper D et al (2016) New brain tumor entities emerge from molecular classification of CNS-PNETs. Cell 164:1060–1072. https://doi.org/10.1016/j.cell.2016.01.015
22. Tomic TT, Olausson J, Wilzen A, Sabel M, Truve K, Sjogren H et al (2017) A new GTF2I-BRAF fusion mediating MAPK pathway activation in pilocytic astrocytoma. PLoS One 12:e0175638. https://doi.org/10.1371/journal.pone.0175638

Affiliations

Damian Stichel[1,2] · Daniel Schrimpf[1,2] · Belén Casalini[1,2] · Jochen Meyer[1,2] · Annika K. Wefers[1,2,3] · Philipp Sievers[1,2] · Andrey Korshunov[1,2,3] · Christian Koelsche[1,2,10] · David E. Reuss[1,2] · Annekathrin Reinhardt[1,2] · Azadeh Ebrahimi[1,2] · Francisco Fernández-Klett[1,2] · Tobias Kessler[4,5] · Dominik Sturm[3,6,7] · Jonas Ecker[3,7,9] · Till Milde[3,7,9] · Christel Herold-Mende[11] · Olaf Witt[3,7,9] · Stefan M. Pfister[3,6,7] · Wolfgang Wick[4,5] · David T. W. Jones[3,8] · Andreas von Deimling[1,2] · Felix Sahm[1,2,3]

1 Department of Neuropathology, Institute of Pathology, University Hospital Heidelberg, Heidelberg, Germany

2 Clinical Cooperation Unit Neuropathology, German Consortium for Translational Cancer Research (DKTK), German Cancer Research Center (DKFZ), Heidelberg, Germany

3 Hopp Children's Cancer Center (KiTZ), Heidelberg, Germany

4 Department of Neurology and Neurooncology Program, National Center for Tumor Diseases, Heidelberg University Hospital, Heidelberg, Germany

5 Clinical Cooperation Unit Neurooncology, German Cancer Consortium (DKTK), German Cancer Research Center (DKFZ), Heidelberg, Germany

6 Division of Pediatric Neurooncology, German Cancer Consortium (DKTK), German Cancer Research Center (DKFZ), Heidelberg, Germany

7 Department of Pediatric Oncology, Hematology, Immunology and Pulmonology, University Hospital Heidelberg, Heidelberg, Germany

8 Pediatric Glioma Research Group, German Consortium for Translational Cancer Research (DKTK), German Cancer Research Center (DKFZ), Heidelberg, Germany

9 CCU Pediatric Oncology, German Cancer Research Center (DKFZ), German Cancer Consortium (DKTK), Heidelberg, Germany

10 Department of General Pathology, Institute of Pathology, Heidelberg University Hospital, Heidelberg, Germany

11 Division of Experimental Neurosurgery, University Hospital Heidelberg, Heidelberg, Germany